PLED devices containing triphenylamine-derived polyurethanes as hole-transporting layers exhibit high current efficiencies†

Cheng-Hsiu Ku,[a] Chao-Hui Kuo,[a] Chih-Yi Chen,[a] Man-Kit Leung[ac] and Kuo-Huang Hsieh*[ab]

Received 15th October 2007, Accepted 3rd January 2008
First published as an Advance Article on the web 29th January 2008
DOI: 10.1039/b715929c

The innovative polyurethane-type polymers from a triphenylamine derivative, [*N*,*N*′-bis(4-hydroxyphenyl)-*N*,*N*′-diphenylbenzidine] (TPA) and a carbazole derivative, [9-butyl-3,6-bis(4-hydroxyphenyl)carbazole] (Cz) can be linked through isophorone diisocyanate (IPDI) bridges and incorporated as hole-transporting layers in high-performance PLED devices. The TPA–IPDI–Cz type of polyurethane (PU) materials (P1–P5) showed superb hole injection and transport properties based on the results of the hole-only-device study. We prepared the devices in two kinds of configuration: system (1) Indium Tin Oxide (ITO)/PU (20 nm)/{Iridium(III) bis(2-phenylpyridine), [Ir(ppy)$_3$] + 2-(4-biphenyl)-5-(4-*tert*-butylphenyl)-1,3,4-oxadiazole (*t*-PBD) + polyvinylcarbazole (PVK)] (50 nm)/Mg (10 nm)/Ag (100 nm), for the device with P1 (DP1), the brightness increased to 14 000 cd m^{-2}, the current efficiency rose to 13.4 cd A^{-1}, and the turn-on voltage was reduced to 21 V (at 100 cd m^{-2}). In system (2) ITO/PEDOT–PSS (30 nm)/PU (20 nm)/[Ir(ppy)$_3$ + *t*-PBD + PVK] (50 nm)/Mg (10 nm)/Ag (100 nm), with PEDOT–PSS as the hole-injection layer, was compared to the standard device (S2) having the configuration ITO/PEDOT–PSS (50 nm)/[Ir(ppy)$_3$ + *t*-PBD + PVK] (50 nm)/Mg (10 nm)/Ag (100 nm); the brightness of the double layer device with P5 (DDP5) increased to 12 500 cd m^{-2} and the current efficiency dramatically rose to 34.7 cd A^{-1}, compared with values of 6250 cd m^{-2} and 21.8 cd A^{-1}, respectively, for S2.

Introduction

In 1990, Friend and coworkers described the first polymeric light-emitting diode (PLED),[1] in which the luminescent poly(*p*-phenylenevinylene) (PPV) was fabricated by spin-coating a precursor polymer onto a transparent conducting indium tin oxide (ITO) anode substrate, thermally converting the precursor into PPV, and then evaporating an Al film cathode onto the PPV layer.

Iridium(III) bis(2-phenylpyridine) [Ir(ppy)$_3$] was one of the earliest developed green-light phosphorescent materials. Ir(ppy)$_3$ is commonly employed for its high external quantum efficiency performance in emitting devices, making them potentially useful as low-power-consumption displays and good diffusive illuminating light sources.[2,3] The excellent light-emitting ability of Ir(ppy)$_3$ results from effective Förster energy transfer between its singlet and triplet states leading to its high external quantum efficiency.[3] The host material is usually Ir(ppy)$_3$ doped with the hole-transporting polymer polyvinylcarbazole (PVK) or the electron-transporting 2-(4-biphenyl)-5-(4-*tert*-butylphenyl)-1,3,4-oxadiazole (*t*-PBD). The energy within this layer is transferred through a series of energy levels, where each successive energy gap is lower and more readily conquered, thus enhancing the performance of the device.

The most widely used hole-transporting materials are triarylamine derivatives because of their relatively high mobilities and low ionization potentials; their hole-transporting rates are *ca.* 1×10^{-3}–10^{-4} cm V s^{-1}.[4–6] Their ability to be used in the spin-coating of large-area electroluminescent (EL) devices and their large range of possible chemical modifications make triarylamines promising hole-transporting materials. Carbazole-based polymers are also drawing increased attention for use in light-emitting devices because of their favorable optical properties and good hole-transporting abilities.[7] A good hole-transporting material must exhibit a high transport rate, high thermal stability, and the ability to be prepared in well-formed films. The basic structural requirements for a hole-transporting material are (1) a non-planar molecular structure to increase the geometrical conformation in the molecules in order to inhibit the formation of π-stacking, (2) functional groups that increase the volume and molecular weight of the molecule, thus enhancing its thermal stability, and (3) rigid groups, such as carbazole moieties, or a combination of intermolecular hydrogen bonds and non-planar molecules to increase the effective molecular weight.[8] There are many structures that display good hole-transporting ability,[6–17] for example, *N*,*N*′-bis(naphthalen-1-yl)-*N*,*N*′-bis(phenyl)benzidine (NPB) is the most widely used hole-transporting material because of its simple synthesis and purification. Shirota, Bettenhausen, Tokito, Jandke, Thelakkat *et al.*[7,11–14] created amorphous triarylamine-based structures exhibiting relatively high thermal stability and durability.

[a]*Institute of Polymer Science and Engineering, National Taiwan University, Taipei, Taiwan, 106*
[b]*Department of Chemical Engineering, National Taiwan University, Taipei, Taiwan, 106*
[c]*Department of Chemistry, National Taiwan University, Taipei, Taiwan, 106*

† Electronic supplementary information (ESI) available: Experimental details and NMR, mass spectral data for compounds **1–6**, PU polymer data collected as UV-Vis, PL, IR spectra and thermo properties as DSC, TGA. PLED device fabrication details and measurements for PU polymers. See DOI: 10.1039/b715929c

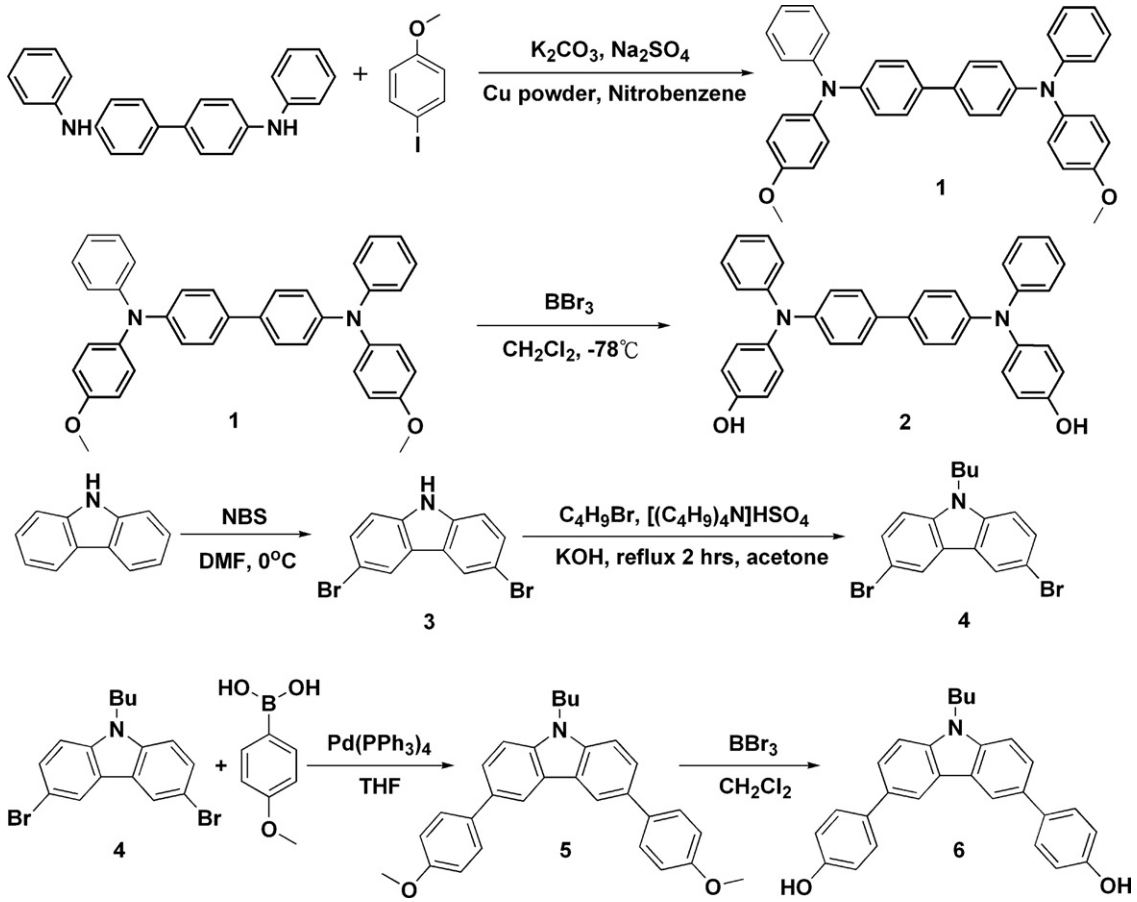

Scheme 1 Synthesis of the diol monomers.

In this present study, we prepared two series of polyurethanes functionalized with triphenylamine-carbazole derivatives. By taking advantage of the well-known hole-injecting ability of triphenylamine systems and the hole-transporting ability of carbazole systems,[18–22] we combined these two components to form a series of polymers exhibiting hole-injecting and hole-transporting ability to replace PEDOT–PSS, the most widely used hole-injection layer (HIL). We chose to synthesize PU derivatives because their polymerization can be performed under metal ion-free conditions, which is an important feature because a low level of metal ion contaminants is an essential requirement for high-performance electronic polymers from pure diols and diisocyanates.[23] The configurations of the PLED devices follow and are separated into two systems for comparison. In system 1, a primitive standard device with ITO/$Ir(ppy)_3$ + PVK + PBD/Mg/Ag (S1), compares PU polymers inserted into ITO and the emitting layer. In system 2, the devices were fabricated in order to compare the hole-transporting capability of the PEDOT and the PU polymers.

Results and discussion

Design of polymer

Our synthesized polyurethanes were of the general type TPA–IPDI–Cz, where carbamate units linked the triphenylamine derivatives (TPA), which are good hole-injecting materials, to the carbazole derivatives (Cz), which are good hole-transporting materials, according to a previous report.[24] We selected the TPA monomer **2** [*N*,*N*′-bis(4-hydroxyphenyl)-*N*,*N*′-diphenylbenzidine] and the Cz monomer **6** [9-butyl-3,6-bis(4-hydroxyphenyl) carbazole] as the basic components to construct PUs that could act simultaneously as both hole-injecting and -transporting layers as potential replacements for the most widely used hole-injecting polymer PEDOT–PSS and possibly improve both the brightness and current efficiency of the resulting devices. To systematically evaluate the performance of the polymers, we synthesized the homopolymer P1 incorporating only the TPA monomer, copolymers P2–P4 at TPA-to-Cz feeding ratios of 3 : 1, 1 : 1, and 1 : 3, respectively, and the homopolymer P5 incorporating only the Cz monomer.

Monomer synthesis

Scheme 1 displays our synthetic route toward the two diol monomers of the PU, monomers **2** and **6**, which played the role of the hole-transporting moiety in the PU. We synthesized monomer **2** in a two-step process. The reaction of *N*,*N*′-diphenylbenzidine with 4-iodoanisole in 1,2-dichlorobenzene at 190 °C for 36 h produced *N*,*N*′-bis(4-methoxyphenyl)-*N*,*N*′-diphenylbenzidine (**1**) in 73% yield after purification. Deprotection of **1** using BBr_3 in CH_2Cl_2 at −78 °C for 2 h provided **2** in 92% yield after column chromotagraphy (CH_2Cl_2–EtOAc, 4 : 1). We synthesized the Cz monomer **6** in four steps. 9*H*-Carbazole was treated with

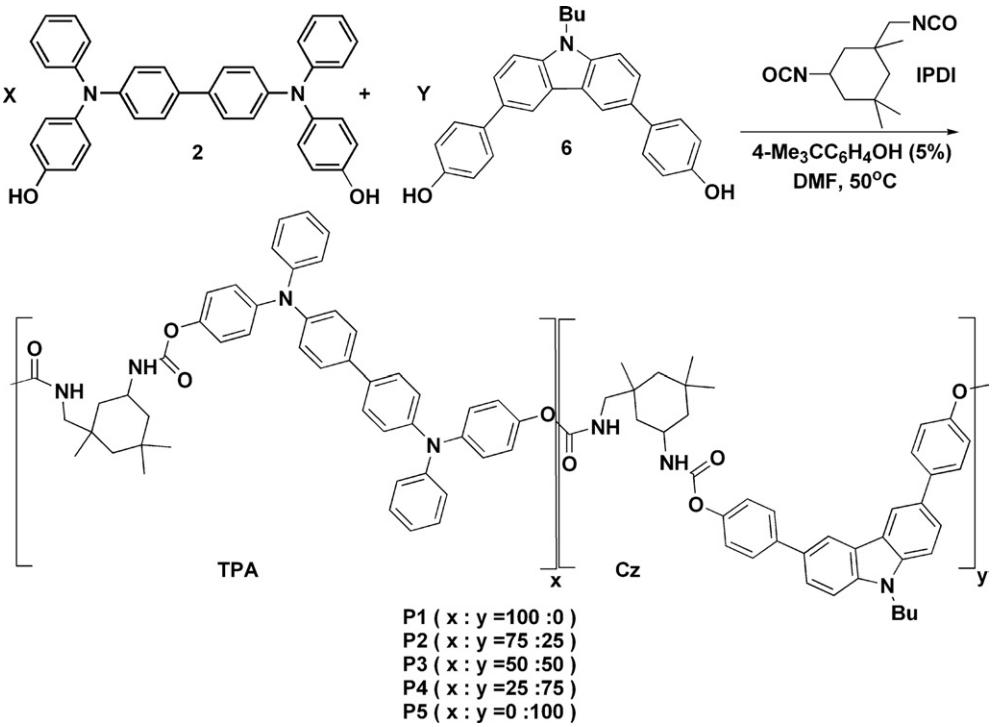

Scheme 2 Synthesis of the TPA–IPDI–Cz (PU) copolymers.

NBS while cooling in an ice bath; recrystallization of the product provided 3,6-dibromo-9*H*-carbazole (**3**) in 92% yield. The reaction of 1-bromobutane with **3** in the presence of a phase transfer agent and base provided 3,6-dibromo-9-butylcarbazole (**4**) in 65% yield. Suzuki coupling of **4** with 4-$MeOC_6H_4B(OH)_2$ yielded 9-butyl-3,6-bis(4-methoxyphenyl)carbazole (**5**). BBr_3-Mediated deprotection of the two terminal methoxy groups of **5** gave the monomer diol **6** in 70% yield.

Synthesis and characterization of polymers P1–P5

We performed the polymerizations of monomers **2** and **6** in dry DMF, using commercially available IPDI as the linker unit, to obtain the TPA–IPDI–Cz copolymers P2–P4 at feeding ratios of 3 : 1, 1 : 1, and 1 : 3, respectively (Scheme 2). We also synthesized the homopolymers P1 and P5 from **2** and **6**, respectively, for comparison.

We obtained molecular weight data (values of M_n, M_w, and PDI) for the prepared polyurethanes using gel permeation chromatography (GPC), analyzing against polystyrene standards in DMF. Table 1 lists these data in addition to the polymers. The values of M_w were stable, ranging from 6000 to 7500, with M_n values from 3600 to 5500, suggesting narrow PDIs. The thermal properties of a polymer are strongly correlated to the performance of its devices. A high value of T_d implies good thermal stability. When a device is fabricated, the materials are evaporated under high vacuum and at high temperature; thus, polymeric materials that have high temperature-stability will improve the life-time of the emitting device. In contrast, a material that is unstable when heated might undergo morphological change, deformation, or degradation of its film, potentially hindering its ability to transport holes and electrons in the device, which would harm the device performance.[25] The values of T_d for our PU derivatives (270–295 °C) were all above the device operation temperature, suggesting that they would be stable under the conditions of thermal evaporation. Among the polymers P1–P5, P4 displayed the highest value of T_d.

Table 1 Thermal properties of polymers P1–P5

Polymer	M_w	M_n	M_w/M_n	T_g/°C	T_d/°C[a]
P1	7500	4800	1.57	174	274
P2	6000	5200	1.16	175	281
P3	7000	5500	1.26	178	285
P4	6200	3600	1.72	174	295
P5	7400	5200	1.42	165	272

[a] The value of T_d corresponds to the 5% weight-loss temperature in TGA.

Optical and electrochemical properties of polymers P1–P5

Fig. 1 displays the optical properties of polymers P1–P5, including their UV-Vis absorption spectra; Table 2 lists the peak maxima from each spectrum. In this series, the homopolymers P1 and P5 and the copolymers P2–P4 exhibited their absorption peak maxima in the region 290–305 nm, which we assign to the π–π* electronic transition contributed by the polymer backbones. We observed no spectral wavelength shifts in the solution spectra, indicating that intra-chain interaction between the TPA and Cz units was minimal. One of the typical peaks of the TPA moiety at 300 nm overlapped with the π–π* transition signal; the intensity of another peak at 350 nm reduced along with the TPA content.[26–28] The typical carbazole absorption peak at 260 nm reduced in intensity along with a decrease in the Cz content,

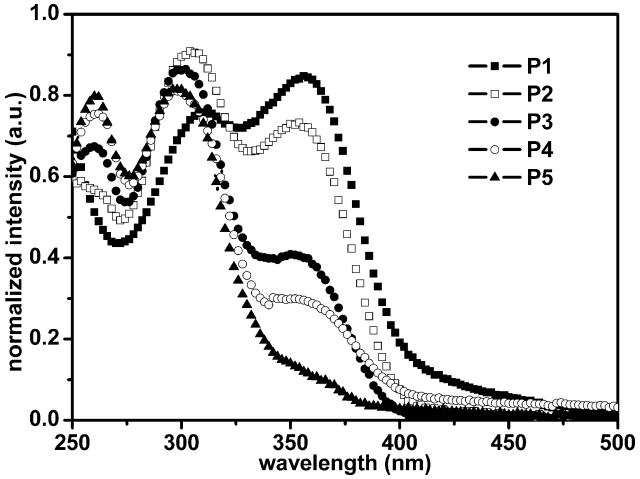

Fig. 1 UV-Vis absorption spectra of PU polymers in THF solution.

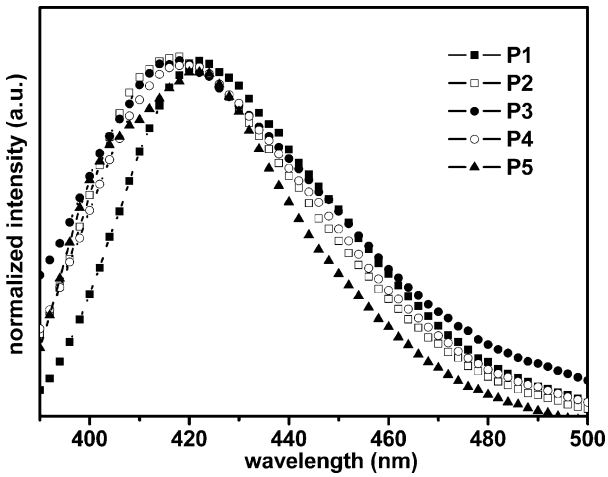

Fig. 2 PL spectra of PU polymer films.

consistent with the polymerizations having been successful at the various TPA-to-Cz feed ratios. Fig. 2 displays the photoluminescence (PL) spectra of P1–P5 as solid films. The peaks all appeared at 420 nm and exhibited similar band widths.

Electrochemical characteristics

For organic electroluminescent materials, the HOMO and LUMO levels are closely related to the ability of electrons and holes to be injected from each electrode, because charge transport is governed by a hopping process involving redox reactions of the charge transport materials. We determined the redox properties of our polymers using cyclic voltammetry (CV), scanning the materials reversibly within the voltage range of their oxidation and reduction potentials. When the applied potential reached the oxidation (or reduction) potential, a redox reaction occurred on the surface of the electrode and a redox current was generated; we determined these onset potentials from the points at which the curves exhibited an ious change in the CV character.[29] Table 2 lists the estimated HOMO and LUMO levels of P1–P5, determined by calibrating to the standard potential of ferrocene (4.8 eV); it also lists the band gap energy ($E_g = E_{HOMO} - E_{LUMO}$) and the band gap was determined by the equation $1241\lambda_{onset(nm)}^{-1}$,[30] where λ_{onset} is the onset absorption wavelength. The HOMO energies were all between 5.15 and 5.30 eV, suggesting that these polymers could be expected to have good hole injection abilities when fabricated into devices. The LUMO energy values of these polymers were between 1.97 and 2.20 eV; thus, their band gap energies were in the range 3.10–3.27 eV.

Electroluminescence properties

We prepared devices in two configurations—(1) ITO/PU (20 nm)/[$Ir(ppy)_3$ + *t*-PBD + PVK] (50 nm)/Mg (10 nm)/Ag (100 nm); (2) ITO/PEDOT–PSS (30 nm)/PU (20 nm)/[$Ir(ppy)_3$ + *t*-PBD + PVK] (50 nm)/Mg (10 nm)/Ag (100 nm) and compared their performance to that of the blank devices S1 and S2, respectively.

System (1): ITO/PU/[$Ir(ppy)_3$ +PVK + *t*-PBD]/Mg/Ag

In system (1), the PU derivatives were spin-coated onto the ITO glass substrate and then the emitting layer was spin-coated on the PU surface; finally, Mg and Ag were vacuum deposited onto the device. A primitive standard device, denoted "S1" and having the configuration ITO/[$Ir(ppy)_3$ + *t*-PBD + PVK] (50 nm)/Mg (10 nm)/Ag (100 nm), was prepared without the PU layer for comparison. The devices, DP1–DP5, were fabricated with the structure ITO/PU (20 nm)/[$Ir(ppy)_3$ + *t*-PBD + PVK] (50 nm)/Mg (10 nm)/Ag (100 nm). Table 3 summarizes the brightness–voltage and current–efficiency–voltage behavior of these devices. Luminescence maxima of 14 000, 9970, 11 800, 9190, and 9240 cd m^{-2} were recorded for devices DP1–DP5, respectively. The maximum current efficiencies of DP1–DP5 were 13.4, 5.5, 12.0, 3.6, and 6.4 cd A^{-1}, respectively, under operating potentials of 22, 18, 22, 19, and 23 V, respectively. Fig. 3 indicates that relative to the standard device S1, the turn-on

Table 2 UV-Vis absorption, electrochemical, and photoluminescence properties of polymers P1–P5 as solid films

Polymer	λ_{absmax}/nm	λ_{PLmax}/nm	E_g/eV	HOMO/eV	LUMO/eV
P1	315, 370 (305, 365)[a]	425 (405)[b]	3.10	5.30	2.20
P2	260, 310, 360 (260, 300, 360)	420 (425)	3.14	5.20	2.06
P3	260, 305, 355 (260, 295, 355)	420 (423)	3.18	5.15	1.97
P4	260, 300, 350 (260, 290, 350)	423 (420)	3.18	5.20	2.02
P5	260, 300 (260, 290)	425 (427)	3.27	5.30	2.03

[a] Values in parentheses represent the value of λ_{absmax}(nm) of the polymer in 5 mg/400 mL in THF solution. [b] Values in parentheses represent the value of λ_{PLmax}(nm) of the polymer in 5 mg/20 mL in THF solution.

Table 3 Performance of polymers in system (1) devices

Device	EL emission λ_{max}/nm	Turn-on voltage at 100 cd m^{-2}/eV	Max. brightness cd m^{-2}/eV	Efficiency (cd A^{-1})/eV
DP1	513	14	14 000/26	13.4/22
DP2	510	17	9970/26	5.5/18
DP3	510	18	11 800/26	12.0/18
DP4	510	14	9190/21	3.6/19
DP5	513	17	9240/23	6.4/23
S1	508	31	296/37	1.1/32

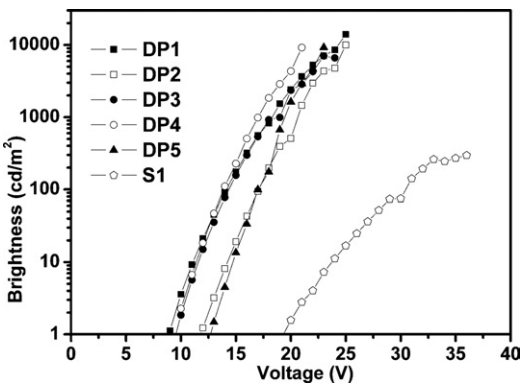

Fig. 3 Brightness–voltage plots for the devices DP1–DP5 and the standard device S1.

voltages, maximum brightness, and maximum efficiencies of DP1–DP5 had improved dramatically. For example, the turn-on voltage of the device incorporating the P1 homopolymer as the hole-injecting layer was reduced to 14 V from 31 V for S1, the maximum brightness increased from 296 cd m^{-2} at 37 V for S1 to 14 000 cd m^{-2} at 26 V for DP1, and the maximum efficiency improved to 13.4 cd A^{-1} at 22 V from 1.1 cd A^{-1} at 32 V for the standard device. DP1 exhibited the best hole-injecting performance in terms of brightness because of the high content of the TPA in the P1 polymer. Fig. 4 presents the current efficiency plotted as a function of the applied voltage for the series of TPA–IPDI–Cz copolymers. The use of the PU layer as both a hole-injecting and -transporting layer on the ITO anode led to significantly improved EL performance relative to that of device S1. DP1–DP5 exhibited significant improvements in brightness as a result of the hole-injecting and -transporting abilities of the TPA and Cz units.

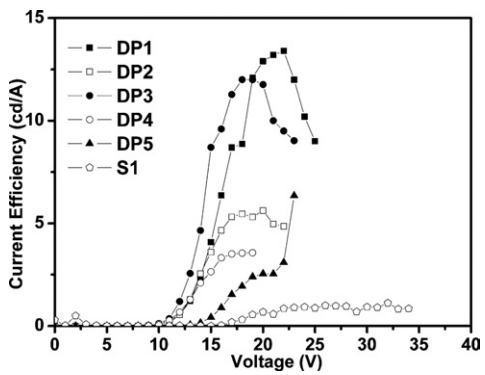

Fig. 4 Current efficiency–voltage plots for devices DP1–DP5 and the standard device S1.

System (2): ITO/PEDOT/PU/[$Ir(ppy)_3$ + PVK + *t*-PBD]/Mg/Ag

In system (2), PEDOT–PSS was first spin-coated onto the glass substrate in DDP1–DDP5 and the standard device S2, followed by the PU hole-injecting and -transporting layer and the emitting layer; the metals Mg and Ag were then evaporation-deposited onto the devices. A double hole-transporting standard device (S2) having the configuration ITO/PEDOT–PSS (30 nm)/[$Ir(ppy)_3$ + *t*-PBD + PVK] (50 nm)/Mg (10 nm)/Ag (100 nm) was prepared for comparison. Table 4 and Fig. 5 and 6 provide the results of brightness–voltage and current efficiency–voltage

Table 4 Performance of polymers in system (2) devices

Device	EL emission λ_{max}/nm	Turn-on voltage at 100 cd m^{-2}/eV	Max. brightness cd m^{-2}/eV	Efficiency (cd A^{-1})/eV
DDP1	511	11	12 500/22	29.4/16
DDP2	506	13	12 100/25	19.6/15
DDP3	507	14	9900/24	17.1/15
DDP4	509	14	10 500/23	21.0/15
DDP5	509	13	8280/24	34.7/17
S2	508	12	6250/22	21.8/15

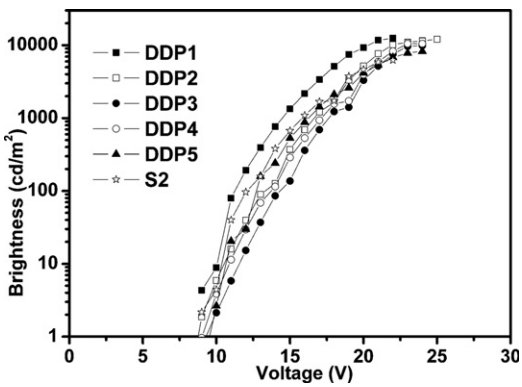

Fig. 5 Brightness–voltage plots for system (2) devices DDP1–DDP5.

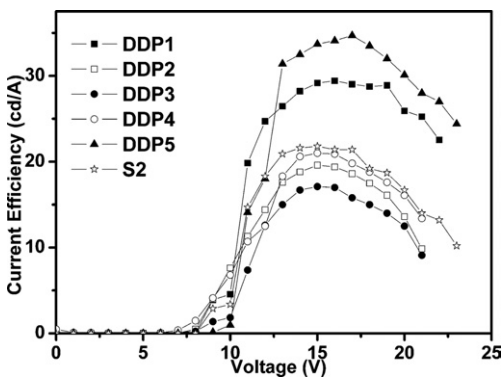

Fig. 6 Current efficiency–voltage plots of system (2) devices DDP1–DDP5.

measurements of the devices. Luminescence maxima of 12 500, 12 100, 9900, 10 500, and 8200 cd m^{-2} were recorded for devices DDP1–DDP5 respectively. The maximum current efficiencies of the devices were 29.4, 19.6, 17.1, 21.0, and 34.7 cd A^{-1} under operating potentials of 16, 15, 15, 15, and 17 V, respectively. Relative to that of the standard device S2 (12.9 cd A^{-1}), the device DDP5 exhibited a significantly improved current efficiency of 34.7 cd A^{-1} as a result of the presence of P5 as the hole-transporting layer. The DDP1 device also displayed a higher current efficiency (29.4 cd A^{-1} at 16 V) than that of the standard device S2 (21.8 cd A^{-1} at 15 V).

The identical green emissions of these devices suggest that they all functioned with identical light-emitting mechanisms and emission zones. We assign the EL peak at 511 nm to the emission from the $Ir(ppy)_3$ + PVK + *t*-PBD emitting layer. Introduction of the PU layer did not alter the emission mechanism. The electroluminescence spectral properties of the PLED devices all retained the same emission wavelength relative to that of the standard device S2.

The accelerated life-time study was conducted at an operating current of 100 mA cm^{-2}. The presence of the PU polymers as hole-transport layers significantly improved the half-life of the device.

Conclusions

We have developed PU polymers and copolymers incorporating triphenylamine and carbazole components linked through IPDI units. Incorporating these PU derivatives as hole-transporting layers in PLED devices greatly improved the performance of the devices; in particular, the use of the triphenylamine PU homopolymer as the hole-transporting layer resulted in outstanding brightness (12 500 cd m^{-2} at 22 V) and superior current efficiency (29.4 cd A^{-1} at 16 V) and carbazole derivative PU polymer, P1, as the hole-transporting layer in DDP5 obtained dramatic high current efficiency (34.7 cd A^{-1} at 17 V). The presence of these PU layers within the devices not only improved the device performance but also maintained the emission color at the same wavelength.

Acknowledgements

This study was supported by the Ministry of Economic Affairs (grant no. 93-EC-17-A-08-S1-0015), the National Science Council of Taiwan, and the Advanced Polymer Nanotechnology Research Center.

References

1 J. H. Burroughs, D. D. C. Bradley, A. R. Brown, R. N. Marks, K. Mackay, R. H. Friend, P. L. Burn and A. B. Holmes, *Nature*, 1990, **347**, 539–541.
2 E. A. Plummer, A. Dijken, H. W. Hofstraat, L. D. Cola and K Brunner, *Adv. Funct. Mater.*, 2005, **15**, 281–289.
3 F. C. Chen, S. C. Chang, G. He, S. Pyo, Y. Yang, M. Kurotaki and J Kido, *J. Polym. Sci., Part B*, 2003, **41**, 2681–2690.
4 B. Chen, C. S. Lee and S. T. Lee, *Jpn. J. Appl. Phys.*, 2000, **39**, 1190–1192.
5 A. Kimoto, J. S. Cho, M. Higuchi and K Yamamoto, *Macromolecules*, 2004, **37**, 5531–5537.
6 U. Bach, K. Cloedt, H. Spreitzer and M Grätzel, *Adv. Mater.*, 2000, **12**, 1060–1063.
7 Y. Shirota, K. Okumoto and H Inada, *Synth. Met.*, 2000, **111**, 387–391.
8 Y. Shirota, T. Kobata and N Noma, *Chem. Lett.*, 1989, 1145–1148.
9 J. Salbeck, N. Yu, Bauer, F. Weissotel and H Bestgen, *Synth. Met.*, 1997, **91**, 209–211.
10 H. Fujikawa, M. Ishii, S. Tokito and Y Taga, *Mater. Res. Soc. Symp. Proc.*, 2000, **621**, Q3.
11 J. Bettenhausen and P Strohriegel, *Adv. Mater.*, 1996, **8**, 507–510.
12 S. Tokito, H. Tanaka, K. Noda, A. Okada and Y Taga, *Macromol. Symp.*, 1997, **125**, 181–185.
13 M. Jandke, P. Strohriegel, S. Berleb, E. Werner and W Brütting, *Macromolecules*, 1998, **31**, 6434–6443.
14 M. Thelakkat and H. W. Schmidt, *Adv. Mater.*, 1998, **10**, 219–223.
15 U. Bach, D. Lupo, P. Compte, J. E. Moser, F. Weissörtel, J. Salbeck, H. Spreitzer and M Grätzel, *Nature*, 1998, **395**, 583–585.
16 G. Yu, J. Gao, J. C. Hummelen, F. Wudi and A. J. Heeger, *Science*, 1995, **270**, 1789–1791.
17 M. Gransröm, K. Petrisch, A. C. Arias, A. Lux, M. R. Anderson and H. R. Friend, *Nature*, 1998, **395**, 257–260.
18 M. Sun, J. Li, B. Li, Y. Fu and Z Bo, *Macromolecules*, 2005, **38**, 2651–2658.
19 S. Jungermann, N. Riegel, D. Müller, K. Meerholz and O Nuyken, *Macromolecules*, 2006, **39**, 8911–8919.
20 G. K. Paul, J. Mwaura, A. A. Argun, P. Taranckar and R. Reynolds, *Macromolecules*, 2006, **39**, 7789–7792.
21 C. W. Ko, Y. T. Tao, J. T. Lin and Thomas, *Chem. Mater.*, 2002, **14**, 357–361.
22 A. Baba, K. Onishi, W. Knoll and R. C. Advincula, *J. Phys. Chem.*, 2004, **108**, 18949–18955.
23 C. H. Kuo, K. C. Peng, L. C. Kuo, K. H. Yang, J. H. Lee, M. K. Leung and K. H. Hsieh, *Chem. Mater.*, 2006, **18**, 4121–4129.
24 J. Li, C. Ma, J. T. Tang, C. S. Lee and S Lee, *Chem. Mater.*, 2005, **17**, 615–619.
25 Z. Peng, Z. Bao and M. E. Galvin, *Chem. Mater.*, 1998, **10**, 2086–2090.
26 A. Baba, K. Onishi, W. Knoll and R. C. Advincula, *J. Phys. Chem.*, 2004, **108**, 18949–18955.
27 E. Bellmann, S. E. Shaheen, S. Thayumanavan, S. Barlow, R. H. Grubbs, S. R. Marder and B Kippelen, *Chem. Mater.*, 1998, **10**, 1668–1676.
28 S. Liu, X. Jiang, H. Ma, M. S. Liu, Jen and K. Y. Alex, *Macromolecules*, 2000, **33**, 3514–3517.
29 L. Liao, Y. Pang, L. Ding and F. E. Karaz, *Macromolecules*, 2004, **37**, 3970–3972.
30 R. Tang, Z. Tan, Y. Li and F. Xi, *Chem. Mater.*, 2006, **18**, 1053–1061.